

Electron-phonon interaction in Ni-Ti

R. Bruinsma

Brookhaven National Laboratory, Upton, New York 11973

(Received 9 November 1981; revised manuscript received 12 January 1982)

The contribution of electron-phonon interaction to the phonon dispersion curve is calculated for Ni-Ti. The anomalies in the dispersion curve are qualitatively reproduced and associated with areas of the Fermi surface having large electron-phonon matrix elements. This provides an understanding of the pre-Martensitic phenomena in Ni-Ti.

The equiatomic transition-metal alloy Ni-Ti has a B_2 structure (CsCl) above room temperature. It undergoes a Martensitic phase transition to what seems, a B_{19} structure at T_m (300 K).¹ Above T_m , x-ray and electron diffraction² show diffuse scattering at $\bar{q}_I = \frac{1}{3}(1, 1, 1)$ with polarization along [111] and at $\bar{q}_{II} = \frac{1}{3}(1, 1, 0)$ with polarization $[\bar{1}10]$, while inelastic neutron scattering³ finds phonon softening at \bar{q}_{II} and a convex curvature in the dispersion curve of the TA modes. In addition there is anomalous temperature dependence of the C_{44} elastic constant.⁴ The relation between the pre-Martensitic phenomena and the Martensitic phase transition is not understood. A 3% addition of Fe, which is substitutional for Ni, suppresses the Martensitic phase transition and a continuous displacive phase transition occurs at 230 K, with a soft phonon at \bar{q}_{II} (but not at \bar{q}_I) producing an incommensurate superlattice with wave vectors near \bar{q}_I and \bar{q}_{II} .⁵ It seems likely then that the Martensitic phase transition has an origin different from the soft modes. Soft modes of type I have been observed in Zr and Ti alloys (ω phase) and are sometimes attributed to formation of a charge density wave,⁶ while soft modes of type II are seen in transition-metal carbides⁷ where they are associated with electron-phonon interaction involving p - d hybridized bands.⁸

For pure Ni-Ti, infrared absorption⁹ indicates the disappearance of large sections of the Fermi surface at the Martensitic phase transition consistent with charge-density wave formation. We will assume then that electron-phonon interaction is responsible for the pre-Martensitic phenomena. A screened Coulomb interaction can be used to understand a *longitudinal* soft mode, but it does not give rise to any transverse anomalies.⁸

A general method for calculating the electron-phonon matrix elements in single basis transition metals was developed by Varma *et al.*¹⁰ Using their method, the anomalous electron-phonon contribution to the phonon dispersion curve may be calculated once the band structure is known. A self-consistent augmented plane wave (APW) calculation was performed by Papaconstantopoulos.¹¹ His calculation was fitted¹² with an orthogonalized tight-binding Hamiltonian involving s , p , and d orbitals on both Ni and Ti, providing 18 electronic levels $\epsilon_\mu(\vec{k})$ with $\mu = 1, 18$ (Fig. 1). The fitting parameters are tabulated in Table I. The rms error at Γ, X, M, R and halfway Δ, Σ , and Δ was 0.7×10^{-3} Ry. The result of Varma *et al.* may be generalized to include a multiple basis. Since Ni-Ti has an inversion center at every atom it is convenient to calculate the modified dynamical ma-

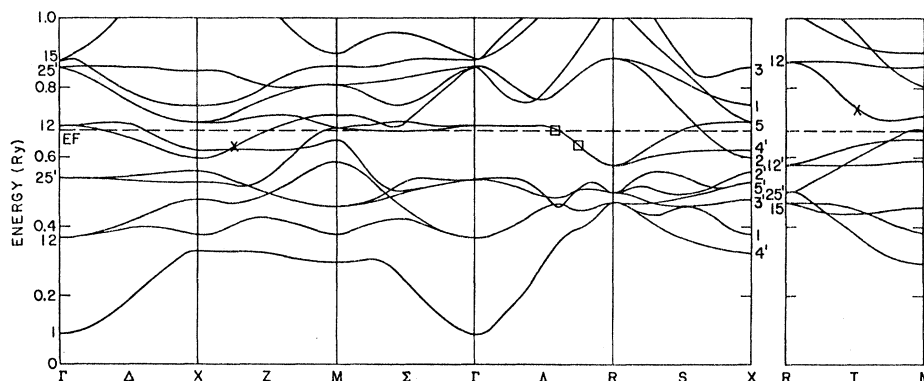


FIG. 1. Band structure produced by a tight-binding fit to Ref. 10. The crosses indicate initial and final points of the dominant scattering contributing to the Σ_4 mode, the squares are initial and final points of scattering contributing to Δ_1 .

TABLE I. Slater-Koster fitting parameters for Ni-Ti (in Ry). The parameters not cited here were determined from the rule $(sp\sigma) = (ss\sigma \times pp\sigma)^{1/2}$.

	Ni-Ni	Ti-Ti	Ni-Ti
E_s	0.582 98	2.4009	
E_p	0.926 84	2.7097	
E_{dt}	0.535 65	0.734 12	
E_{de}	0.536 89	0.737 25	
$ss\sigma$	-0.073 48	0.150 73	-0.048 27
$pp\sigma$	0.106 16	-0.143 54	0.062 31
$pp\pi$	-0.062 79	-0.062 77	0.204 07
$dd\sigma$	-0.018 10	-0.044 27	-0.045 62
$dd\pi$	0.006 81	0.028 64	0.031 08
$dd\delta$	0.000 84	-0.004 00	-0.005 00

trix, which is real and symmetric in this case. The modified dynamical matrix is defined as

$$C_{\alpha\beta}(\kappa, \kappa' | \vec{q}) = \frac{1}{\sqrt{M_\kappa M_{\kappa'}}} \sum_l \Phi_{\alpha\beta}(0, \kappa | l, \kappa') \times \exp[i\vec{q} \cdot (\vec{R}_l + \vec{x}_{\kappa'} - \vec{x}_\kappa)] \quad (1)$$

where l runs over all unit cells. The matrix $\Phi_{\alpha\beta}$ gives the force constant between atom κ with position \vec{x}_κ and mass M_κ and atom κ' with position $\vec{R}_l + \vec{x}_{\kappa'}$ and mass $M_{\kappa'}$.

The second-order electron-phonon contribution to the modified dynamical matrix is

$$C_{\alpha\beta}^{(2)}(\kappa, \kappa' | \vec{q}) = \frac{1}{\sqrt{M_\kappa M_{\kappa'}}} \sum_{\substack{\mu=1,18 \\ \mu'=1,18}} g_{\alpha,\kappa}^{\mu,\mu'}(\vec{k}, \vec{k} + \vec{q}) g_{\beta,\kappa'}^{*\mu,\mu'}(\vec{k}, \vec{k} + \vec{q}) \frac{f_\mu(\vec{k}) - f_{\mu'}(\vec{k} + \vec{q})}{\epsilon_\mu(\vec{k}) - \epsilon_{\mu'}(\vec{k} + \vec{q})} \quad (2)$$

with $\kappa=1$ for Ni and $\kappa=2$ for Ti and $f_\mu(k)$ is the Fermi distribution function. The electron-phonon matrix element is given as

$$g_{\alpha,\kappa}^{\mu,\mu'}(\vec{k}, \vec{k} + \vec{q}) = q^2 \sum_{n=1,9} A_{\mu,\kappa n}^+ (\vec{k}) A_{n\kappa,\mu} (\vec{k} + \vec{q}) [v_\mu^\alpha(\vec{k}) - v_{\mu'}^\alpha(\vec{k} + \vec{q})] \quad (3)$$

where $A_{n\kappa,\mu}(\vec{k})$ is the 18×18 unitary eigenvector matrix of the tight-binding Hamiltonian and $v_\mu^\alpha(\vec{k})$ is $\partial \epsilon_\mu / \partial k_\alpha$. The coefficient q^2 is given by

$$q^2 = 4/a^2 \quad (4)$$

where a is the lattice constant (3 Å). This relation assumes that overlap integrals vary with distance as $1/R^2$. The result of the calculation is shown in Fig.

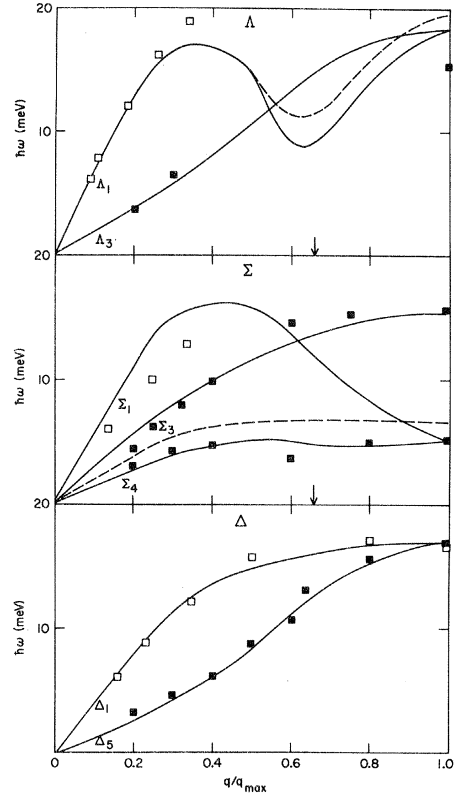


FIG. 2. Phonon dispersion curves along Δ , Σ , and Λ . The experimental points are those of Bührer *et al.* (\square longitudinal mode, \blacksquare transverse mode). The dotted lines indicate the short-range contribution to Δ_1 and Σ_4 . The arrows indicate the position of the wave vectors of the superlattice which appears below 230 K in Ni-Ti (Fe).

2. The short-range force constants [1 NN (nearest neighbor) and 2NN] were determined by a least-square fit to the BZ boundary phonon frequencies and the sound velocities. In usual notation, $F_{\alpha\beta}^{1NN}(1, 2) = A \delta_{\alpha\beta} + B(1 - \delta_{\alpha\beta})$; $F_{xx}^{2NN}(\kappa, \kappa) = A_\kappa$; $F_{yy}^{2NN}(\kappa, \kappa) = F_{zz}^{2NN}(\kappa, \kappa) = B_\kappa$; $F_{xy}^{2NN}(\kappa, \kappa) = 0$, they were in units of 10^4 dyn/cm: $A = 0.78$, $B = 1.83$, $A_1 = 0.35$, $B_1 = 0.18$, $A_2 = 6.15$, and $B_2 = -0.18$. Along Σ , the modified dynamical matrix has the fol-

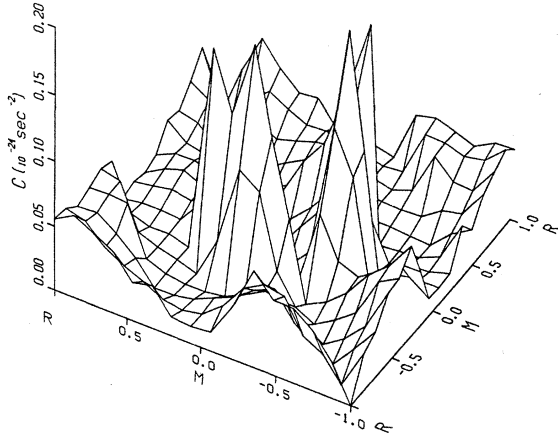


FIG. 3. Electron-phonon contribution to the dynamical matrix $C \equiv C_5^{(2)}(\vec{q}) - C_4^{(2)}(\vec{q})$ with phonon wave vector $\vec{q} = 0.31(1, 1, 0)2\pi/a$ and polarization $[\bar{1}10]$ (Σ_4). The electronic wave vector is restricted to the RXM plane.

lowing general form:

$$C_{\alpha\beta}(1, 1|\vec{q}) = \begin{bmatrix} C_1(\vec{q}) & C_2(\vec{q}) & 0 \\ C_2(\vec{q}) & C_1(\vec{q}) & 0 \\ 0 & 0 & C_3(\vec{q}) \end{bmatrix} \text{ (Ni-Ni) ,} \quad (5a)$$

$$C_{\alpha\beta}(2, 2|\vec{q}) = \begin{bmatrix} C_4(\vec{q}) & C_5(\vec{q}) & 0 \\ C_5(\vec{q}) & C_4(\vec{q}) & 0 \\ 0 & 0 & C_6(\vec{q}) \end{bmatrix} \text{ (Ti-Ti) ,} \quad (5b)$$

$$C_{\alpha\beta}(1, 2|\vec{q}) = \begin{bmatrix} C_7(\vec{q}) & C_8(\vec{q}) & 0 \\ C_8(\vec{q}) & C_7(\vec{q}) & 0 \\ 0 & 0 & C_9(\vec{q}) \end{bmatrix} \text{ (Ni-Ti) .} \quad (5c)$$

The anomaly in Σ_4 is caused by the large electron-phonon contribution to $C_4(\vec{q}) - C_5(\vec{q})$. Note that this only involves interactions between Ti atoms. The electron-phonon contribution $C \equiv C_5^{(2)}(\vec{q}) - C_4^{(2)}(\vec{q})$ has a maximum along Σ at $\vec{q}_M \approx 0.31 \times (1, 1, 0)2\pi/a$, close to \vec{q}_{II} . The maximum is caused by a large contribution from the region around $\vec{k} = (0.13, -0.06, -0.5)2\pi/a$ to the summation in Eq. (1). In Fig. 3(a) the contributions to C in the $k_x = -\pi/a$ plane are plotted for $\vec{q} = \vec{q}_M$. The peak is caused by a transition from a Z_1 level to a T_1 level, both with large $\nu_\mu(\vec{k})$ (Fig. 1). Both levels are $d_{x^2-y^2}$ levels localized on Ti, with only little p -wave

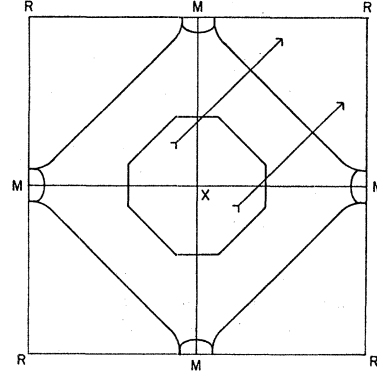


FIG. 4. Fermi surface in the RXM plane. Arrows indicate the dominant scattering producing the anomaly in Σ_4 .

admixture, contrary to the conclusion of Ref. 8. The energy transfer is 0.11 Ry.

The anomaly in Λ_1 is caused by a maximum along Λ in $C(\vec{q}) \equiv -[C_7^{(2)}(\vec{q}) + 2C_8^{(2)}(\vec{q})]$ at $\vec{q}_M \approx 0.25(1, 1, 1)2\pi/a$ which is, again, close to q_{II} , and again only involving Ti-Ti force constants. The maximum is due to large contributions from the regions around $\vec{k} \approx 0.27(1, 1, 1)2\pi/a$ and $\vec{k} \approx (-0.12, -0.12, 0.4)2\pi/a$.

In the first case the transition is from a Λ_3 level to the same level with an energy transfer of 0.03 Ry. This is a d level involving both Ni and Ti atoms. In the second case the transition is from a S_4 level to a Λ_3 level with an energy transfer of 0.02 Ry. The S_4 level and Λ_3 level are d levels localized on Ti. The pre-Martensitic phenomena in Ni-Ti (Fe) thus seem due to formation of a gap on the electron pocket centered at X (Fig. 4) and the flat Fermi surface along Λ .

As was mentioned, a 3% addition of Fe to pure Ni-Ti causes the phonon anomalies to produce a superlattice at $T \approx 230$ K. Within the rigid-band model no appreciable effect was found on the phonon anomalies. The Fe impurities possibly cause local strains contributing to the central peak above 230 K observed in neutron scattering.¹³

ACKNOWLEDGMENTS

I am indebted to S. Shapiro for suggesting the problem and for valuable discussions. I gratefully acknowledge useful conversations with J. Davenport, M. Salamon, S. Satija, and J. Watson. I would like to thank M. Salamon and S. Shapiro for a critical reading of the manuscript. I am grateful to D. Papaconstantopoulos for allowing me to use his unpublished band-structure calculation. The work was supported by DOE under Contract No. DE-AC02-76CH00016.

- ¹D. P. Dautovich and G. R. Purdy, *Can. Metall. Q.* **4**, 129 (1965).
- ²K. Chandra and G. R. Purdy, *J. Appl. Phys.* **30**, 2176 (1968). R. F. Hehemann and G. D. Sandrock, *Scr. Metall.* **5**, 801 (1971).
- ³W. Bühner, O. Mercier, P. Bruesch, and R. Gotthard, *Prog. Rep.* 1980, E.T.H., AF-SSP-115 (Zürich, 1981), p. 60.
- ⁴O. Mercier, K. N. Melton, G. Gremaud, and J. Hagi, *J. Appl. Phys.* **51**, 1833 (1980).
- ⁵M. B. Salamon, M. Meichle, C. M. Wayman, C. M. Hwang, and S. M. Shapiro, in *Modulated Structures—1979 (Kailua Kona, Hawaii)*, edited by J. M. Cowley, J. B. Cohen, M. B. Salamon, and B. J. Wuensch, AIP Conf. Proc. No. 53 (AIP, New York, 1979), p. 223; S. K. Satija, S. M. Shapiro, and M. B. Salamon, *Bull. Am. Phys. Soc.* **26**, 381 (1981); M. E. Meichle, M. B. Salamon, and C. M. Wayman, *ibid.* **26**, 381 (1981).
- ⁶R. Pynn, *J. Phys. F* **8**, 1 (1978); A. L. Simons and C. M. Varma, *Solid State Commun.* **35**, 317 (1980).
- ⁷H. G. Smith, *Phys. Rev. Lett.* **29**, 353 (1972).
- ⁸W. Hanke, J. Hafner, and H. Bilz, *Phys. Rev. Lett.* **37**, 1560 (1976).
- ⁹I. I. Sasovskaya, S. A. Shabalovskaya, and A. I. Lotkov, *Zh. Eksp. Teor. Fiz.* **77**, 2461 (1979) [*Sov. Phys. JETP* **50**, 1128 (1979)].
- ¹⁰C. M. Varma and W. Weber, *Phys. Rev. B* **19**, 6142 (1979); *Phys. Rev. Lett.* **39**, 1094 (1977).
- ¹¹D. A. Papaconstantopoulos (unpublished).
- ¹²J. C. Slater and G. F. Koster, *Phys. Rev.* **94**, 1498 (1954); D. A. Papaconstantopoulos, B. M. Klein, J. S. Faulkner, and L. L. Boyer, *Phys. Rev. B* **18**, 2784 (1978).
- ¹³S. Shapiro (private communication).